
Figures and figure supplements

A facile approach for the in vitro assembly of multimeric membrane transport proteins

Erika A Riederer *et al*

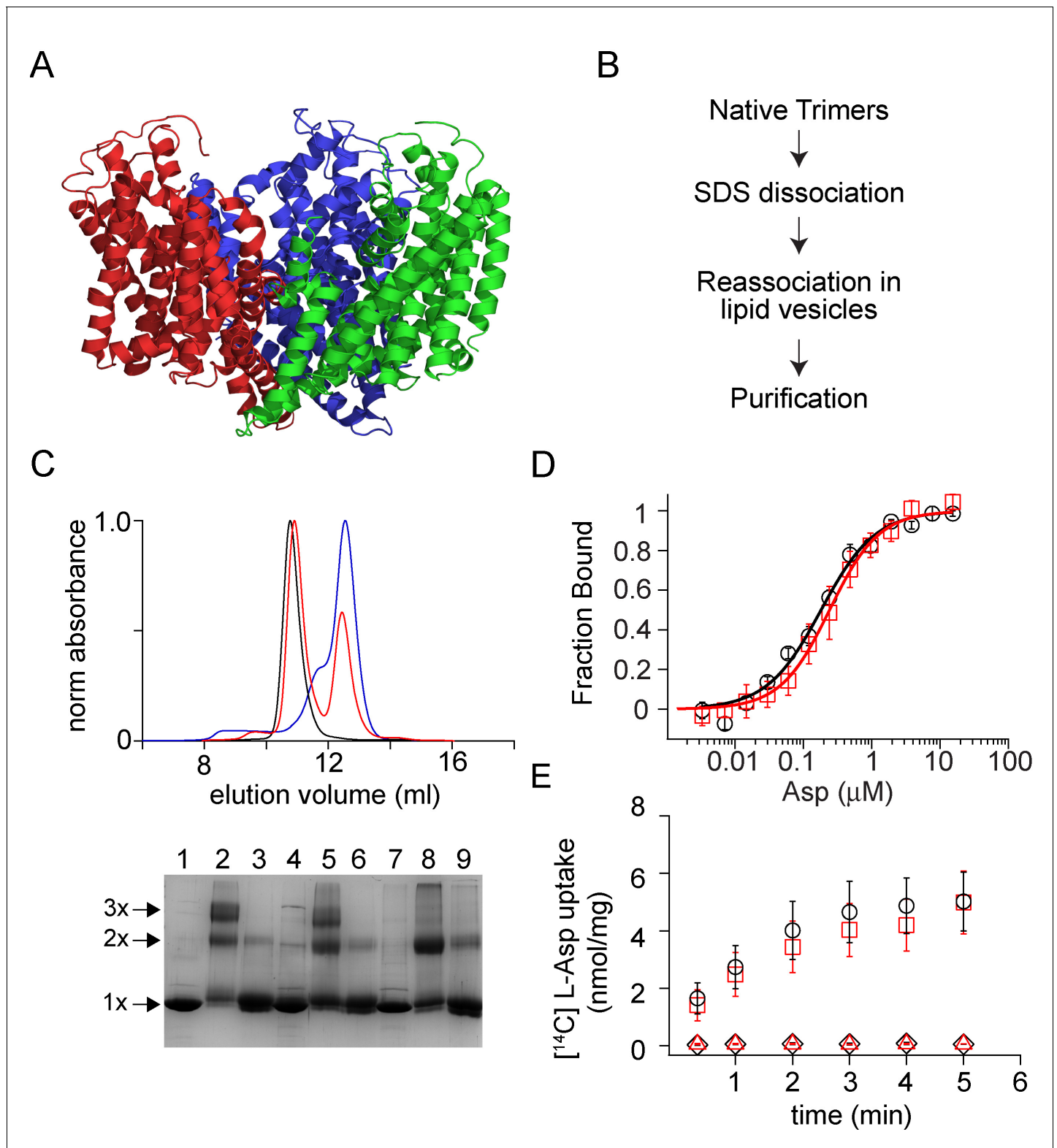


Figure 1. Dissociation and reassociation of Glt_{Ph}. (A) Structure of the Glt_{Ph} trimer (pdb: 2nwx) is shown in ribbon representation. (B) Flow chart outlining the strategy used for the dissociation and reassociation of the Glt_{Ph} trimer. (C) Size exclusion chromatography of the native Glt_{Ph} (black) and the SDS dissociated Glt_{Ph} following dilution into lipid vesicles (red) and into DDM (blue). Reassembly of Glt_{Ph} takes place in lipid vesicles. Inset, SDS-PAGE gel showing the glutaraldehyde crosslinking of the native Glt_{Ph} (lanes 1–3), reassociated Glt_{Ph} (r-Glt_{Ph}, lanes 4–6) and the SDS dissociated Glt_{Ph} subunits (lanes 7–9). Lanes 1, 4, and 7, without glutaraldehyde crosslinking, lanes 2, 5, and 8, with glutaraldehyde crosslinking and lanes 3, 6, and 9, with glutaraldehyde crosslinking. Figure 1 continued on next page

Figure 1 continued

glutaraldehyde crosslinking in the presence of 1% SDS. The oligomeric nature of the protein band (1x, 2x, and 3x) is indicated. (D) Asp binding by native and r-Glt_{Ph}. Asp binding was monitored by changes in fluorescence of the native (black circles) or r-Glt_{Ph} (red squares) with the L130W substitution. The fraction of the protein bound (F_{bound}) is determined by dividing the change in fluorescence upon addition of Asp by the total change at the end of the titration. Solid lines are fits to the data using the equation described in Materials and methods with K_D values of 183 ± 16 nM for native Glt_{Ph} and 216 ± 15 nM for r-Glt_{Ph}. The binding assays were conducted in 10 mM Na⁺. (E) Asp uptake assay. The time course of [¹⁴C]-Asp uptake for native Glt_{Ph} (black circles) and r-Glt_{Ph} (red squares) in the presence of a Na⁺ gradient. No uptake is observed for native Glt_{Ph} (black diamonds) and r-Glt_{Ph} (red triangles) in the absence of a Na⁺ gradient. For panels D and E, error bars indicate standard error of mean (SEM) for $n \geq 3$.

DOI: <https://doi.org/10.7554/eLife.36478.002>

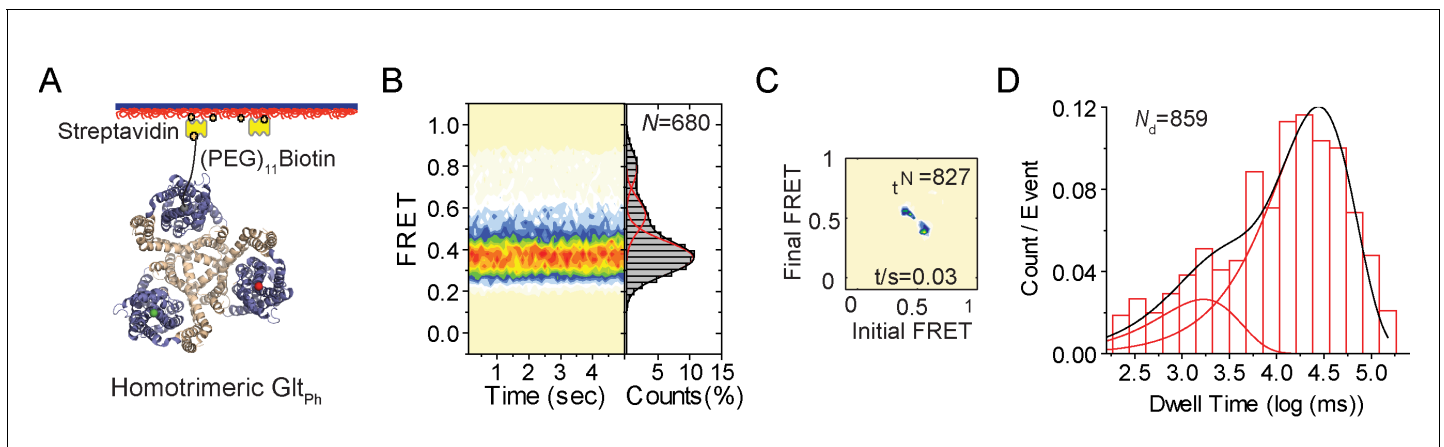


Figure 2. smFRET experiments on reassociated Glt_{Ph} molecules. (A) Labeling and surface-immobilization strategy for smFRET experiments. (B) Population distributions FRET efficiency population contour plots (left) and cumulative population histograms (right) are shown for r-Glt_{Ph}. The contour plots are color-coded from tan (lowest) to red (highest population) with the color scale from 0–12%. The population histograms display the time-averaged values and standard deviations. The solid black lines are fits to the sums of individual Gaussian functions (red lines). The number of molecules analyzed (N) is shown. (C) Transition density plots show that transitions occur at a frequency of ~0.03/ s. The number of transitions in the dataset (N_t) is shown. (D) Dwell time distribution for the low-FRET state obtained for r-Glt_{Ph} shows biphasic behavior and was fitted to a probability density function. The number of dwells in the analysis (N_d) is shown.

DOI: <https://doi.org/10.7554/eLife.36478.003>

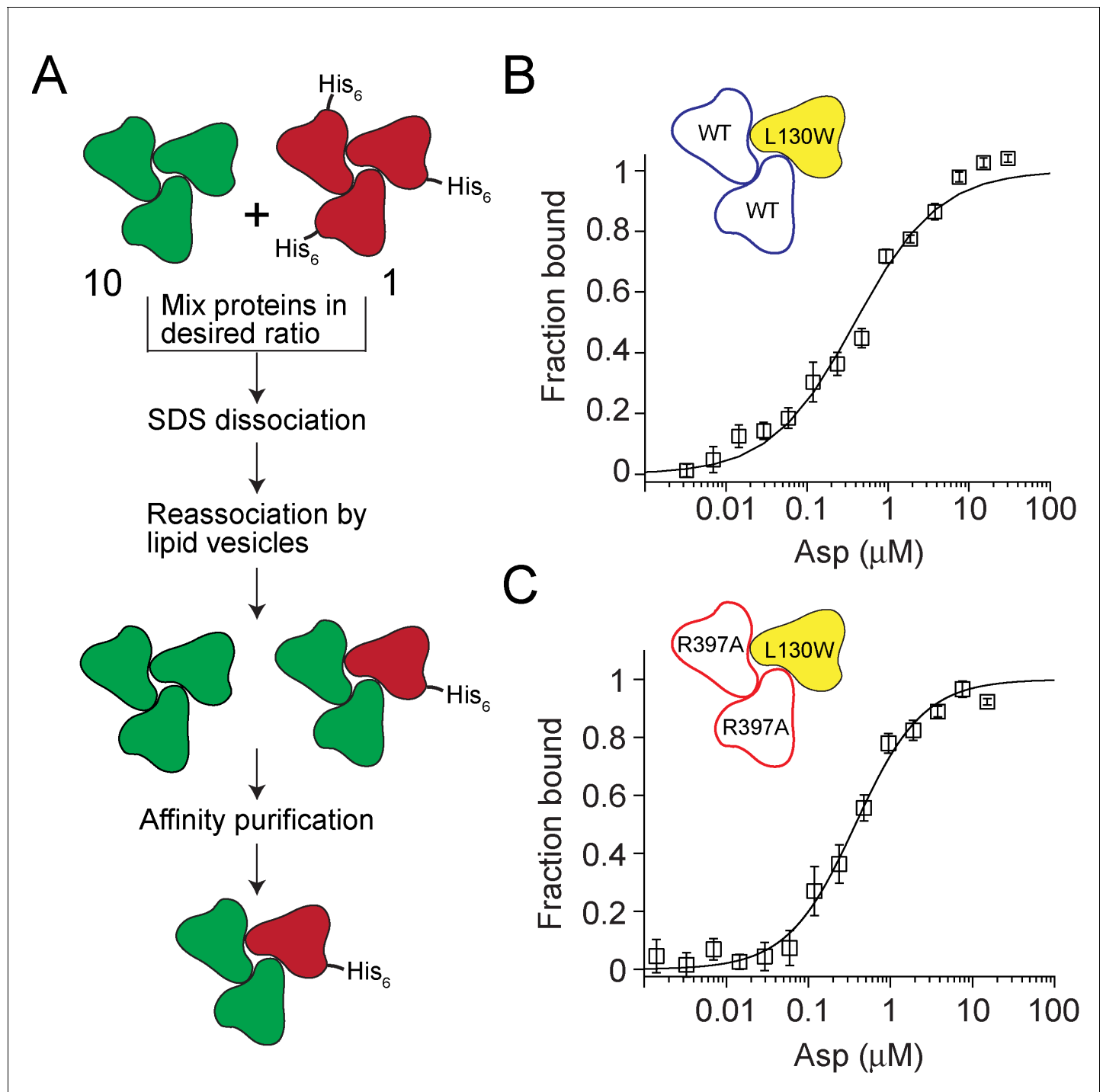


Figure 3. Testing crosstalk between Glt_{Ph} subunits in Asp binding. **(A)** Flowchart outlining the strategy used for assembling heterotrimers of Glt_{Ph}. The test subunits are depicted in green and the reporter subunits are in red. A 10: 1 ratio of test to reporter subunits is used to ensure that the probability of assembling heterotrimers with more than one reporter subunit is very low. The presence of a polyhistidine tag on the reporter subunit enables purification of the heterotrimers that contain a reporter subunit. **(B and C)** Asp binding to heterotrimeric Glt_{Ph} with test subunits containing the wild-type Asp-binding site (blue, **B**) or with a R397A substitution in the Asp binding site (red, **C**). The reporter subunit (yellow) contains the L130W substitution for monitoring Asp binding to the subunit. Asp-binding assays as described in **Figure 1D**. The solid lines indicate fits to the data using a Hill equation with $K_D = 455 \pm 61$ nM, Hill coefficient = 0.84 ± 0.08 for the heterotrimer with the wild-type test subunits and with $K_D = 356 \pm 36$ nM, Hill coefficient = 1.05 ± 0.07 for the heterotrimer with test subunits carrying the R397A substitution. Error bars indicate SEM for $n \geq 3$.

DOI: <https://doi.org/10.7554/eLife.36478.004>

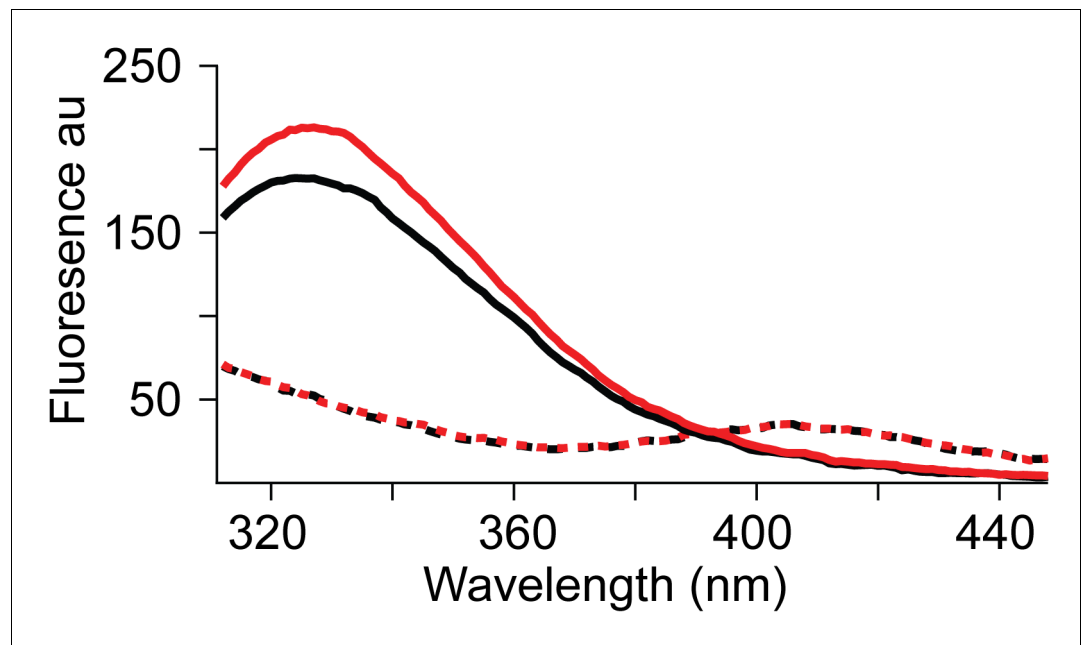


Figure 3—figure supplement 1. Spectral properties of wild type and L130W Glt_{Ph}. Fluorescence emission spectra of the L130W Glt_{Ph} in 10 mM NaCl (solid black) and after addition of 100 μM Asp (solid red) with excitation at 295 nm. Spectra of the wild-type Glt_{Ph} before (dashed black) and after the addition of 100 μM Asp (dashed red). Equal amounts (50 nM) of the wild type and the L130W Glt_{Ph} protein was used for measuring the spectra. An increase in fluorescence at 334 nm is observed on Asp binding by L130W Glt_{Ph}. No corresponding fluorescence change is observed for the wild-type Glt_{Ph}.

DOI: <https://doi.org/10.7554/eLife.36478.005>

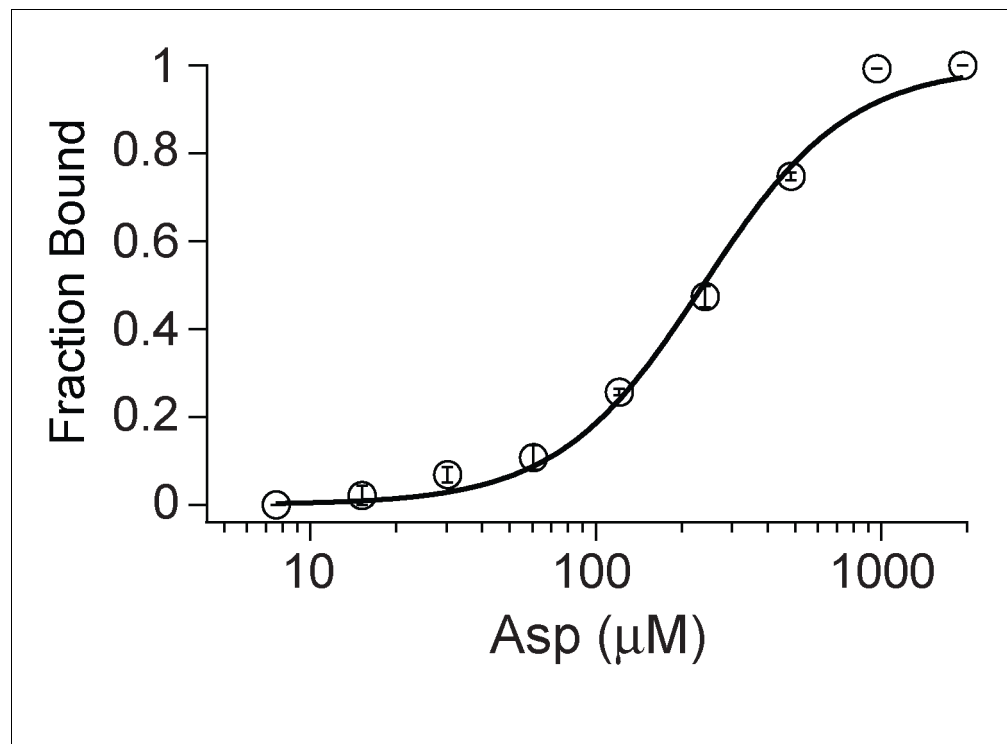


Figure 3—figure supplement 2. Asp binding by R397A Glt_{Ph}. Asp binding by R397A Glt_{Ph} with the L130W substitution in 10 mM Na⁺ was carried out as described in legend to **Figure 1**. The R397A substitution ($K_D = 238 \mu\text{M}$) causes a ~ 1300 fold decrease in affinity for Asp binding compared to the wild-type Glt_{Ph} ($K_D = 0.183 \mu\text{M}$). Error bars indicate SEM for $n \geq 3$.

DOI: <https://doi.org/10.7554/eLife.36478.006>

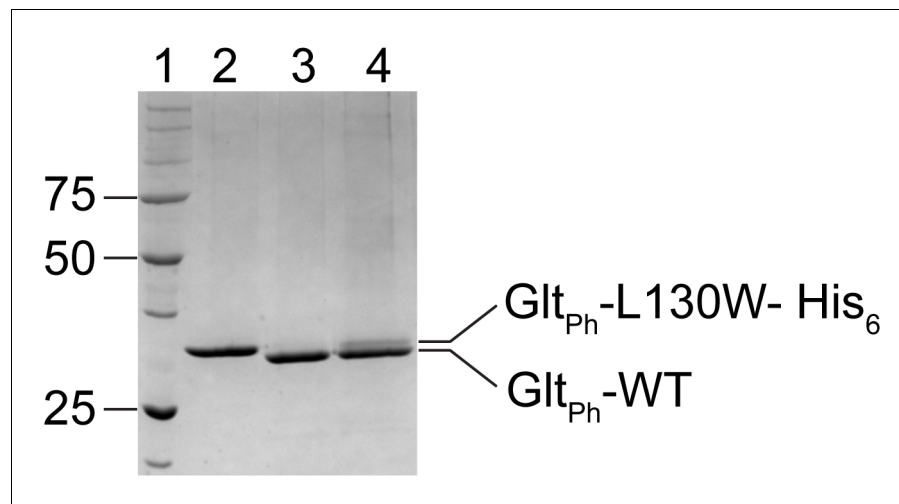


Figure 3—figure supplement 3. Assembly of heteromeric Glt_{Ph} . A heteromeric Glt_{Ph} with two wild-type subunits and one subunit with the L130W substitution was assembled using the protocol diagrammed in **Figure 3A**. SDS-PAGE gel showing molecular weight markers (Lane 1), the L130W Glt_{Ph} His₆ (lane 2), wild type Glt_{Ph} (Lane 3) and heterotrimeric Glt_{Ph} (Lane 4). The presence of both the subunits in the heterotrimeric Glt_{Ph} is shown.

DOI: <https://doi.org/10.7554/eLife.36478.007>

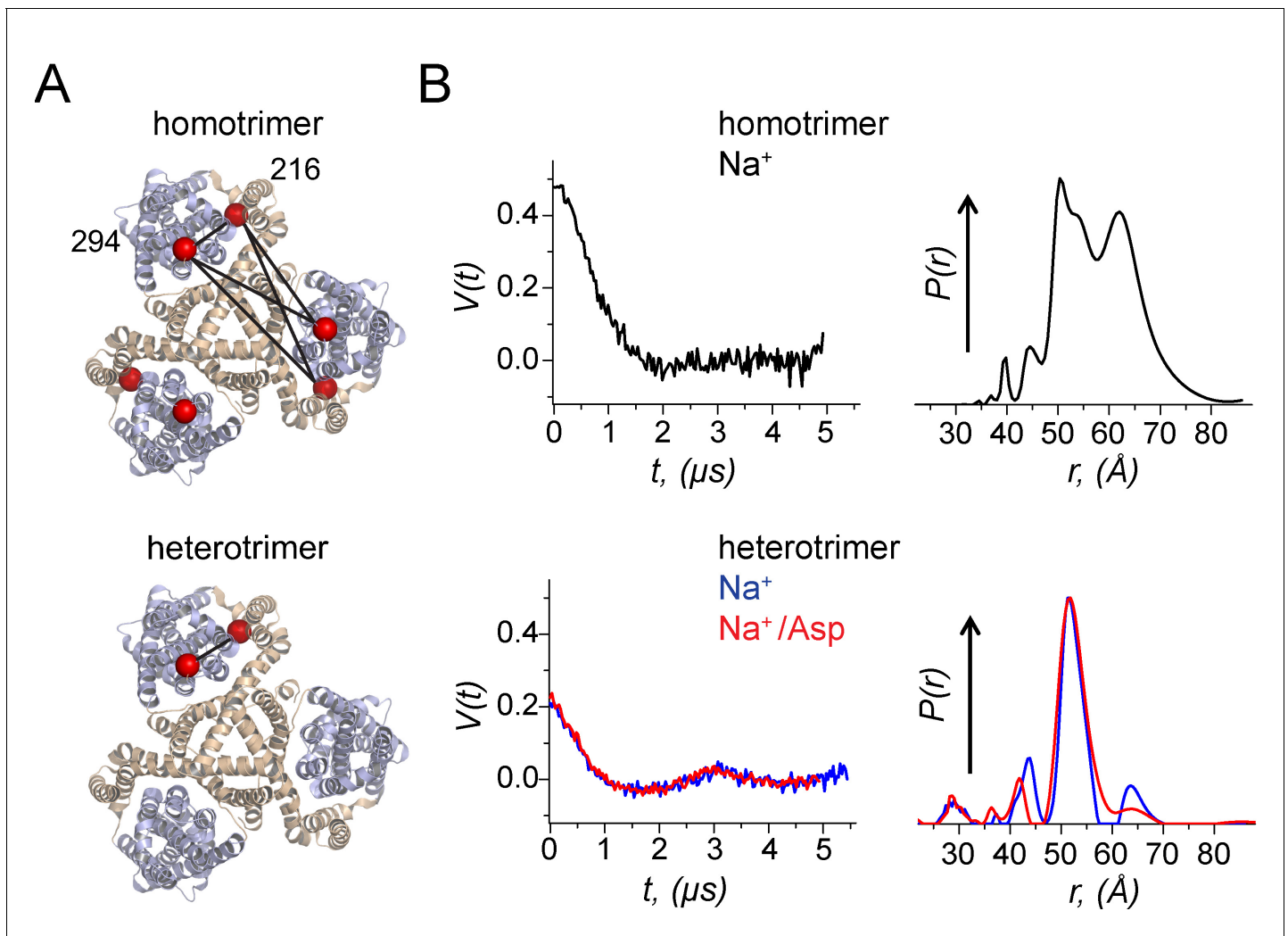


Figure 4. Using a heterotrimeric Glt_{Ph} to probe movements of the transport domain using DEER. (A) A homomeric and a heteromeric Glt_{Ph} transporter are shown in ribbon representation. The scaffold domain is colored in wheat while the transport domain is colored in light blue. The C_β atoms of the Cys residues at 216 and 294 labelled with spin probes are shown as red spheres. All subunits in the homomeric Glt_{Ph} carry the Cys substitutions while only one subunit in the heteromeric Glt_{Ph} carries the Cys substitutions. The distances monitored in the DEER experiment are indicated by solid lines. (B) Background-corrected DEER amplitude, $V(t)$ vs. evolution time t (left). The data are shown for: Glt_{Ph} homotrimers with spin labels at both positions in each of the protomers prepared with 200 mM NaCl (black); Glt_{Ph} heterotrimer with spin-labels just in one of the protomers prepared with either 200 mM NaCl (blue) or 200 mM NaCl/300 μM aspartate (red). The data are plotted to have the 'DEER modulation depth' at $t = 0$ and decay to zero value asymptotically (see Materials and methods). Larger modulation depth, that is $V(0)$ indicates larger number of coupled spins. Inter-spin distance distributions, $P(r)$, reconstructed from the above DEER data, are plotted in respective colors (right). All $P(r)$'s were normalized to common value at the maxima. Glt_{Ph} heterotrimers show much simpler $P(r)$ as compared to convoluted result for homotrimers.

DOI: <https://doi.org/10.7554/eLife.36478.008>

A

GltPh MGLYRK^YIEY^PVLQKIL^IGLIL^IGAIVGL^ILGHYGAHAVHTYV^KPFGLFVRL^LKMLVMP 60
 GltSM MGEWES^YKRF^PVIIYKVAIAFVL^IGI^VAGV^IVGPP-----IAV^IKPLGDVLI^RLLKMI^VVP 54

GltPh IVFASLVVGAASISPARLGRVGVKIVVYLLTSAFAVTLGIIMARLFNPGAGIHLAVGGQ 120
 GltSM IVLFSLVVGSA^SISPLKLGKVGK^II^VY^IVTSAIAVLI^GIA^MGLLFQPGVGVHLAGTCY 114

GltPh QFQPHQAPPLVHI^LLDIVPTNPF^GALANGV^LPTIFFAI^LLGIAIT^YLMNSENEK^VRKSA 180
 GltSM SVKTVTPPSPIDV^LLNIIPTNPWAALVNCN^VLQI^IFFAI^VLGIALAY^LKDSK^DERL^RNLG 174

GltPh ETLLDAINGLA^EAMYKIVN^GVMQY^ABICGVFALIA^VMAEQGVH^VVGELAKVTA^AVYVGLT 240
 GltSM STVLNVFDGLA^EAIYKIVR^GILEY^MPGV^FALIGYAV^AITGPGV^LGPLGVAVV^ALYLGLF 234

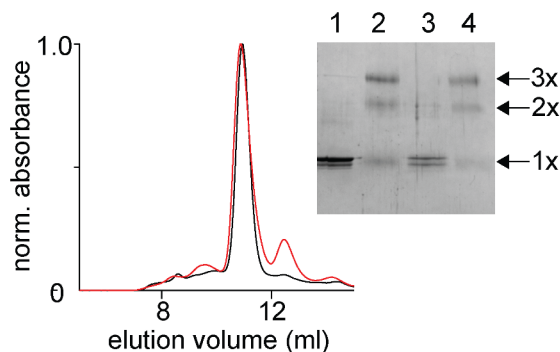
GltPh LQILLV^YFVLLKIYGIDPIS^EFIKHA^KDAMLTAFVTRSSSGTLPV^TMRVAK^E-MGISEGI^Y 299
 GltSM IHIFATYGSILAVFRFNI^IKELAK^ADAMLTAFVTRSSSGTLP^ITMSVA^EEKMGIKKS^IY 294

GltPh SFTLPLGATINMDGTALYQGVCTFFFIANALGSHLTVGQQLTIVLTAVLASIGTAGVPGAG 359
 GltSM AFTLPLGATINMDGTAMYQAIATMFIANALGTHLTVVHYGMIVLTAVLASIGTAGVPGAG 354

GltPh AITMLAMVLHSVGLPLTDPNVAAAYAMILGIDA^IILDMGRMTMVNVTGDLTGTAIVAKTE^GTL 419
 GltSM LITMLALVLQAVGLPLTEPNVALAYSIL^IAGIDV^IILDMGRMTMVNVTGDLTGTLIVAKTE^NET 414

GltPh -VP--R 422
 GltSM DLSKWK 420

B



C

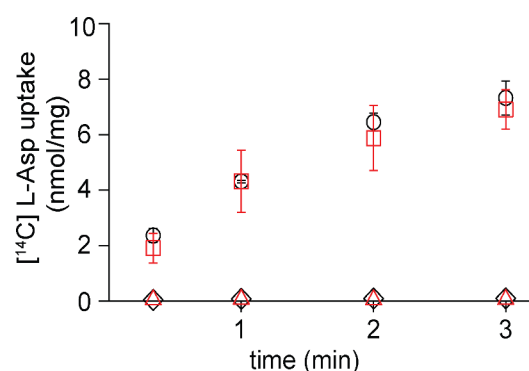


Figure 5. In vitro assembly of Glt_{Sm}. (A) Sequence alignment of Glt_{Sm} with Glt_{Ph} with identical residues highlighted. (B) Size exclusion chromatography of the native (black) and the reassociated Glt_{Sm} (r-Glt_{Sm}, red). Inset, SDS-PAGE gel shows the glutaraldehyde cross-linking of the native and r-Glt_{Sm}. Native Glt_{Sm} without (lane 1) and with glutaraldehyde crosslinking (lane 2) and r-Glt_{Sm} without (Lane 3) and with glutaraldehyde crosslinking (Lane 4) are shown. The oligomeric nature of the protein band (1x, 2x, and 3x) is indicated. (C) Aspartate uptake assay. The time course of [¹⁴C]-Asp uptake by native Glt_{Sm} (black circles) and r-Glt_{Sm} (red squares) in the presence of a Na⁺ gradient. No uptake is observed for native Glt_{Sm} (black diamonds) and r-Glt_{Sm} (red triangles) in the absence of a Na⁺ gradient. Error bars indicate SEM for n ≥ 3.

DOI: <https://doi.org/10.7554/eLife.36478.009>

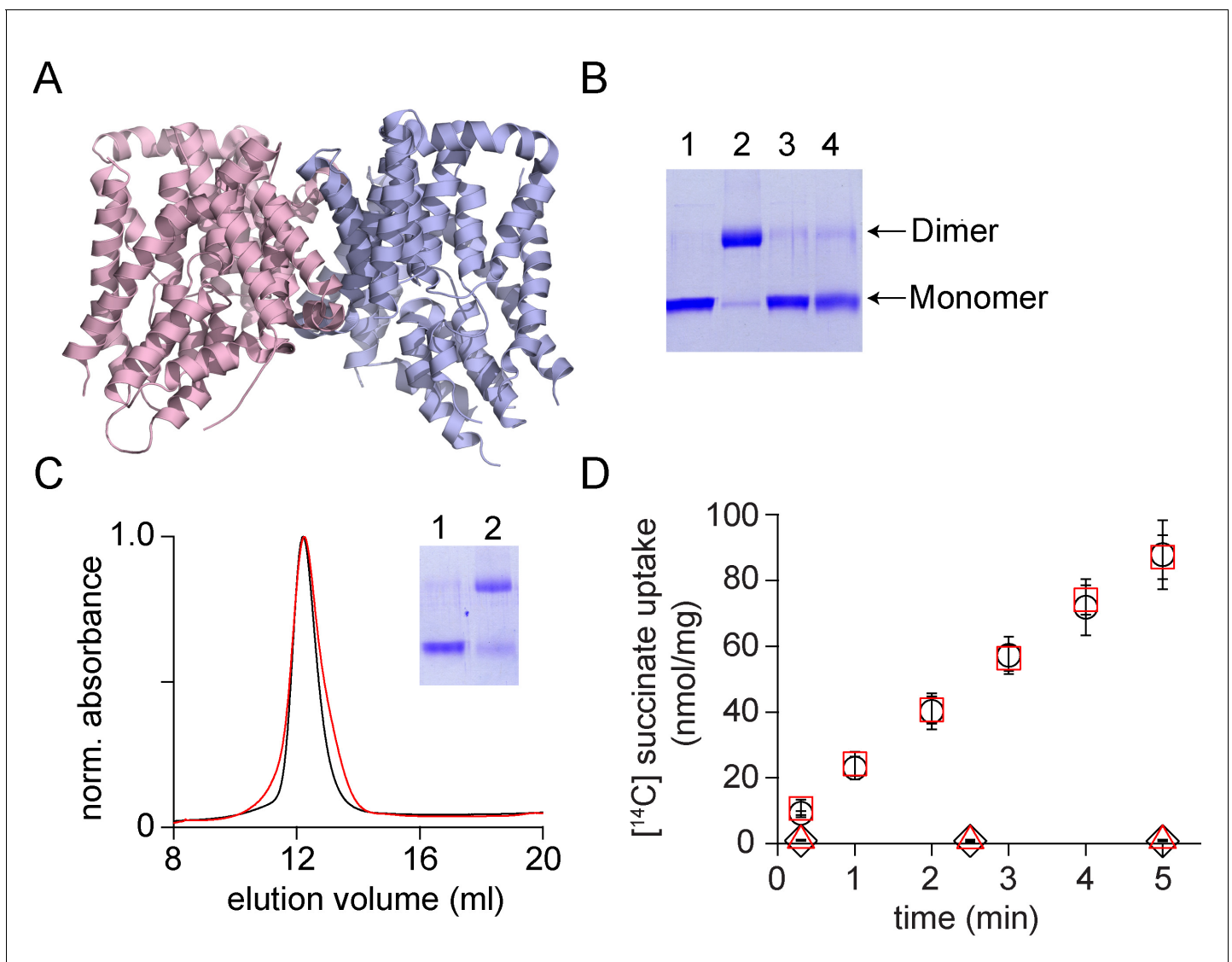


Figure 6. In vitro assembly of VcINDY. (A) Structure of VcINDY (pdb: 4f35) is shown in ribbon representation. (B) Dissociation of the VcINDY dimer by SDS. SDS-PAGE gel showing the native VcINDY without (lane 1), with glutaraldehyde crosslinking (lane 2) and the SDS dissociated VcINDY without (lane 3) and with glutaraldehyde crosslinking (lane 4). (C) Size exclusion chromatography of the native (black) and the reassociated VcINDY (r-VcINDY, red). Inset, SDS-PAGE gel showing the glutaraldehyde cross-linking of the peak fraction of r-VcINDY without (lane 1) and with glutaraldehyde crosslinking (lane 2). (D) Succinate uptake assay. The time course of [^{14}C]-succinate uptake by native VcINDY (black circles) and r-VcINDY (red squares) in the presence of a Na^+ gradient. No uptake is observed for native VcINDY (black diamonds) and r-VcINDY (red triangles) in the absence of a Na^+ gradient. Error bars indicate SEM for $n \geq 3$.

DOI: <https://doi.org/10.7554/eLife.36478.010>

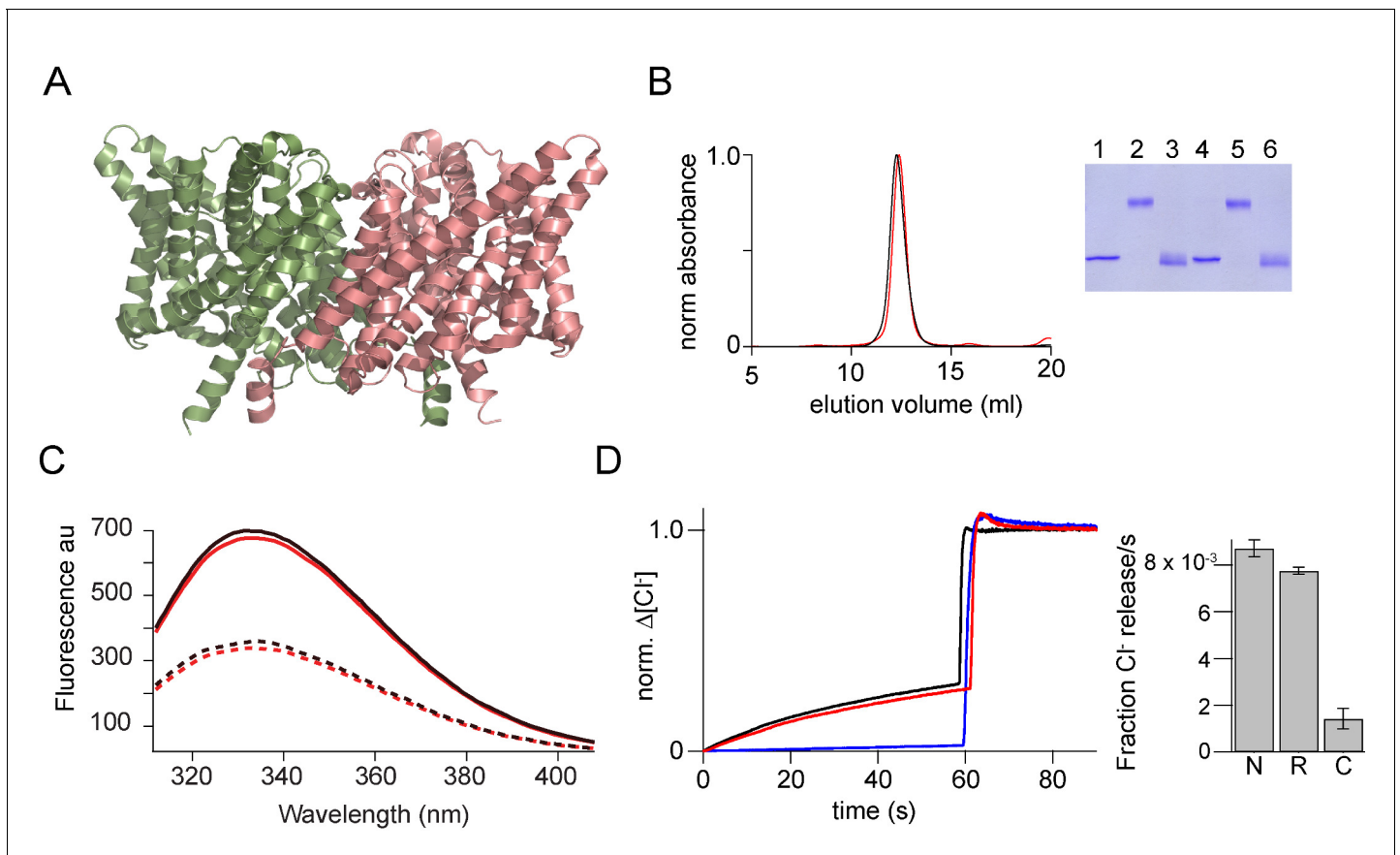


Figure 7. In vitro assembly of CLC-ec1. **(A)** Structure of CLC-ec1 (pdb: 1kpl) shown in ribbon representation. **(B)** Size exclusion chromatography of the native (black) and the in vitro assembled CLC-ec1 (r-CLC-ec1, red). Inset, SDS-PAGE gel showing the glutaraldehyde cross-linking of the peak fraction of native and r-CLC-ec1. Native CLC-ec1 without glutaraldehyde crosslinking (lane 1), with glutaraldehyde crosslinking before (lane 2) and after (Lane 3) treatment with 1% SDS. r-CLC-ec1 without glutaraldehyde crosslinking (lane 4), with glutaraldehyde crosslinking before (lane 5) and after (Lane 6) treatment with 1% SDS. **(C)** Fluorescence spectra of the native and r-CLC-ec1. Intrinsic fluorescence spectra (excitation at 295 nm) for the native (solid black) and r-CLC-ec1 (solid red) in 50 mM Tris-HCl, pH 7.5, 200 mM NaCl, 0.25% DM. Dashed lines show the fluorescence spectra for the native (dashed black) and r-CLC-ec1 (dashed red) after the addition of 1% SDS. **(D)** Chloride transport assays. Left: Chloride efflux from liposomes containing native CLC-ec1 (Black), r-CLC-ec1 (red), and no protein control (blue). Bulk efflux was initiated at time zero by the addition of valinomycin. Triton X-100 was added after 60 s to release all of the intra-vesicular chloride. Chloride efflux was normalized to the total chloride concentration upon addition of Triton X-100. Right: Bar graph showing the normalized rate of chloride movement through liposomes containing native CLC-ec1 (N), r-CLC-ec1 (R), and no protein control (C). Normalized rates were calculated from the initial slope after addition of valinomycin from graphs such as those shown on the left. Error bars represent the SEM from six independent flux assays.

DOI: <https://doi.org/10.7554/eLife.36478.011>